BMC Veterinary Research

CASE REPORT

Open Access

Primary pulmonary histiocytic sarcoma with nodal and esophageal metastasis in a dog—imaging and anatomopathological aspects

Anna Vitória Hörbe[1*], Felipe Auatt Batista de Sousa[1], Catherine Konrad Nava Calva[2], Luna Silvestri Souto[3], Raquel Baumhardt[4], Fabiano da Silva Flores[1], Camila Borghetti[3], Igor Cezar Kniphoff da Cruz[5] and Ricardo Pozzobon[5]

Abstract

Background This report presents a case of esophageal and nodal metastasis in a primary pulmonary histiocytic sarcoma in a dog. Histiocytic sarcoma is a malignant neoplasm originating from histiocytic cells, characterized by its aggressive nature, high metastatic potential and high mortality rate. Pulmonary involvement occasionally results in pleural effusion and regional lymph node involvement, such as the tracheobronchial, sternal, and mediastinal lymph nodes. Thoracic radiography is the preferred complementary diagnostic test when respiratory disorders are suspected, as it can identify pulmonary masses and associated complications, such as pleural effusion. Similarly, ultrasonography can be used when pulmonary conditions are suspected, helping to differentiate lesions.

Case presentation A one-year-old, intact male mixed-breed dog weighing 18 kg was referred for emergency clinical care due to severe inspiratory dyspnea. Thoracic radiography and ultrasonography revealed a large intrathoracic mass located in the mediastinum, displacing adjacent structures, along with associated pleural effusion. The primary diagnostic hypothesis was a neoplasm of cranial mediastinal origin. During the thoracocentesis procedure, the animal decompensated and died. Necropsy revealed a large, multilobulated tumor mass in the mediastinum, showing direct extension into the esophagus, as well as another nodule similar to the mediastinal mass in the left caudal lung lobe. Histopathological analysis supported the diagnosis of pulmonary histiocytic sarcoma with esophageal and nodal metastasis, confirmed through an immunohistochemical panel.

Conclusions The involvement of cranial mediastinal and tracheobronchial lymph nodes, as well as the presence of pleural effusion, are common features associated with HS. However, the occurrence of esophageal metastases is considered uncommon, highlighting the uniqueness of this case, as well as supporting the potential for its occurrence. Thoracic radiography and ultrasonography played a crucial role in the initial suspicion of neoplasia, emphasizing their importance in early diagnostic approaches.

Keywords Lung neoplasia, Mediastinal neoplasia, Metastasis, Radiology, Ultrasonography

*Correspondence:
Anna Vitória Hörbe
annvithorbe@gmail.com

Full list of author information is available at the end of the article

Background

Primary pulmonary neoplasms are rare in dogs, accounting for approximately 1% of canine neoplasms, with most being of malignant origin [1]. Histiocytic sarcoma (HS) is a malignant neoplasm originating from histiocytic cells, such as dendritic cells and macrophages, which are found in various parts of the body [2]. This condition is characterized by its aggressive nature, high metastatic potential, and high mortality rate [3]. It predominantly affects young to middle-aged dogs, typically between the ages between 2 and 10 years, with no sex predisposition, and is more common in breeds such as Bernese Mountain Dogs, Flat-Coated Retrievers, and, more recently, Schnauzers [2, 4, 5].

HS can be classified as hemophagocytic, localized, or disseminated [4, 6]. It predominantly affects the skin or subcutaneous tissue, spleen, liver, lungs, and lymph nodes, but may also involve bones and joints [3]. Pulmonary involvement commonly results in pleural effusion and regional lymph node compromise, such as the tracheobronchial, sternal, and mediastinal lymph nodes [4]. The most frequent clinical signs in these cases include lethargy, anorexia, weight loss, dyspnea, and cough [1, 3].

Thoracic radiography is the preferred complementary diagnostic test when respiratory disorders are suspected, as it can identify pulmonary masses and associated complications, such as pleural effusion [7]. Similarly, ultrasonography is an accessible method that can be used when pulmonary conditions are suspected, helping to differentiate lesions [8]. The definitive diagnosis is based on histopathological examination associated with immunohistochemistry, as the wide range of morphological characteristics observed in these tumors requires immunophenotypic evaluation to confirm the origin of dendritic cells [2].

Primary pulmonary histiocytic sarcoma (HS) in dogs can metastasize locally to the lungs and intrathoracic lymph nodes, as well as distantly to abdominal organs [9]. Involvement of the nervous system has also been reported, including metastases to spinous processes and the spinal cord [10]. While a case of primary esophageal HS has been previously described in a dog [11], esophageal metastasis originating from a primary pulmonary HS, as observed in the present case, has not been documented in the literature. This report aims to describe a case of primary pulmonary HS with esophageal and nodal metastases in a dog, emphasizing the imaging and pathological findings.

Case presentation

A one-year-old, intact male mixed-breed dog weighing 18 kg, was referred to the University Veterinary Hospital of Santa Maria as an emergency case due to dyspnea. During anamnesis, the owner reported that the animal had shown signs of fatigue and dyspnea with any physical effort over the past few weeks. On physical examination, severe inspiratory dyspnea, orthopneic posture, cyanotic mucous membranes, and muffled cardiac and respiratory auscultation were noted. The respiratory rate was 48 breaths per minute, pulse rate was 80 beats per minute, and rectal temperature was 37.7 °C. Additionally, the animal exhibited a low body condition score (cachexia). Intravenous access and oxygen therapy were immediately initiated for stabilization at the beginning of the consultation. After respiratory improvement, complementary diagnostic tests, including hematological examinations and thoracic radiography, were performed.

Hematological tests revealed mild leukocytosis (20,100/mm^3 – reference: 6,000–17,000/mm^3) due to neutrophilia (16,884/mm^3 – reference: 3,000–11,500/mm^3) and monocytosis (2,412/mm^3 – reference: 150–1,350/mm^3), with other parameters within reference values. Radiographic examination was performed using a GE XR-6000 X-ray machine, manufactured by General Eletric, equipped with a wireless imaging system. Thoracic radiographs were obtained using 90 kilovolts (kV) and 2.0 milliampere-seconds (mAs) in a horizontal beam projections, included right and left lateral and dorsoventral views, revealing the presence of a homogeneous, soft-tissue radiopaque intrathoracic mass with slightly irregular contours and large dimensions, measuring approximately 16.9 cm × 8.15 cm × 8.8 cm (length × height × width), located in the dorsal aspect of the cranial and middle mediastinum, displacing the trachea and esophagus dorsally, along with associated pleural effusion, characterized by the accumulation of radiopaque fluid within the pleural space (Fig. 1). To further aid in diagnosis, the patient was referred for thoracic ultrasonography.

The scan was performed using a GE Healthcare LOGIQ F6 ultrasound system, manufactured by General Eletric, with a 10 MHz microconvex transducer, with the patient in right lateral recumbency, covering the third to sixth intercostal spaces on the left side. Due to respiratory distress, the examination was conducted quickly. A heterogeneous and hypoechoic mass was observed cranial to the cardiac silhouette, in the mediastinum, along with moderate, markedly cellular pleural effusion (Fig. 2). The imaging findings were highly suggestive of a cranial mediastinal neoplasia. Although less likely given the clinical context, granulomatous diseases were also considered as differential diagnoses.

Considering the concomitant presence of pleural effusion, the dog underwent thoracocentesis, during which a 23G scalp vein catheter was inserted into the right 8th intercostal space at the mid-thoracic region, yielding a moderately turbid, slightly reddish fluid. The sample was submitted for laboratory analysis, which confirmed a high-cellularity aseptic exudate, ruling out infectious

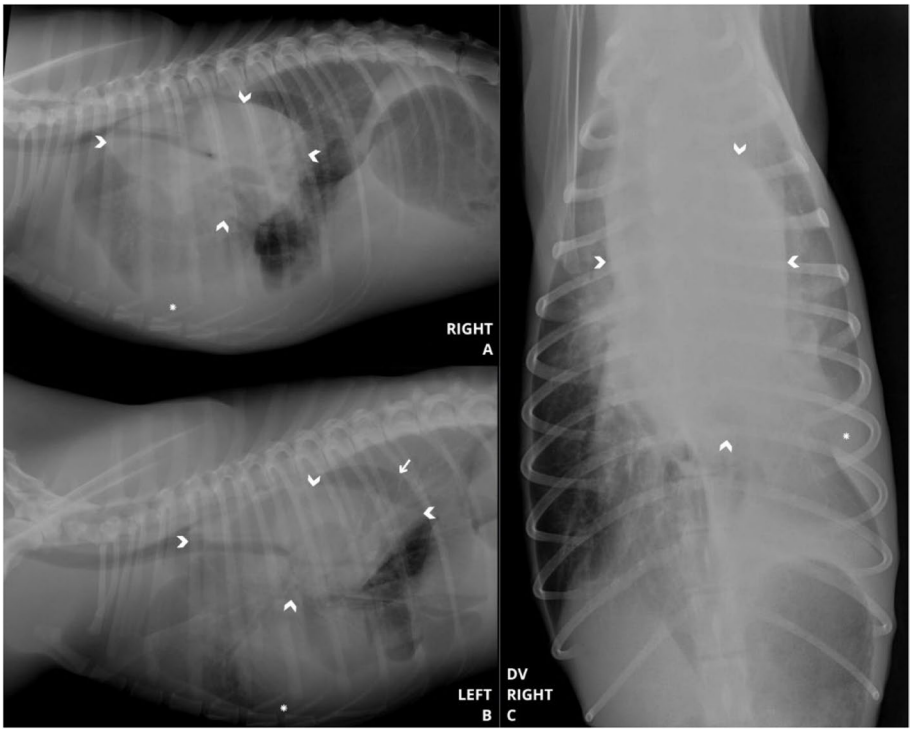

Fig. 1 Thoracic radiographic examination in right lateral (**A**), left lateral (**B**), and dorsoventral (**C**) projections. Increased soft tissue radiopacity is observed in the dorsal aspect of cranial and middle mediastinum (arrowhead) with a mass effect. There is displacement of the thoracic trachea to the right, with dorsal deviation of its cranial portion and ventral deviation of its pre-terminal portion. The esophagus is visible in its cranial portion due to slight distension by gas content, displaced dorsally (arrow). Additionally, the presence of pleural effusion (*) is noted. DV = dorsoventral

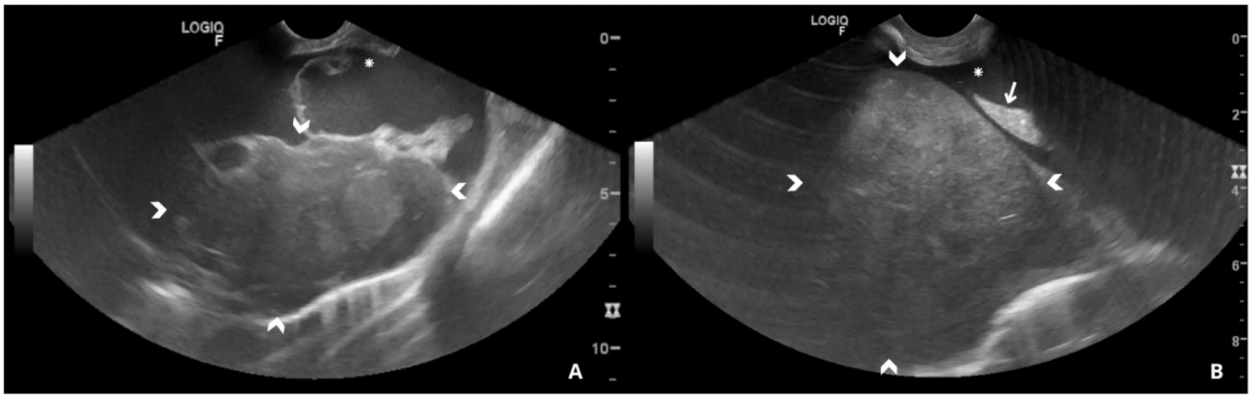

Fig. 2 Thoracic ultrasonographic examination using a microconvex transducer (10 MHz) and scanning between the third and sixth intercostal spaces on the left side. A heterogeneous, hypoechoic (relative to the atelectatic lung) mass with interspersed amorphous echogenic areas, well-defined yet slightly irregular margins, is observed cranial to the cardiac silhouette in the mediastinum (arrowhead). Additionally, a moderate amount of a hypoechoic pleural effusion with a marked presence of gravity-dependent cellular debris (*) and pulmonary lobe atelectasis (arrow) is noted

causes and suggesting a possible neoplastic origin. The cellular composition predominantly consisted of round cells (94%) with high atypia, along with occasional intact neutrophils (6%), suggesting lymphoma as a differential diagnosis. Approximately 600 mL of pleural fluid was drained; however, the patient decompensated during the procedure and, due to cardiopulmonary arrest, died. The body was submitted for pathological examination the same day.

On necropsy, a large, multilobulated tumor mass was observed in the cranial and middle mediastinum, measuring 14.0 cm × 6.0 cm × 8.5 cm (length × height × width), with a firm consistency, whitish coloration, and a homogeneous, smooth cut surface. The mass was associated with severe local lymphadenomegaly and exhibited continuity with the esophagus (Fig. 3A), as well as partial adherence to adjacent lung lobes. On the caudal surface of the left caudal lung lobe, a focal, extensive, firm,

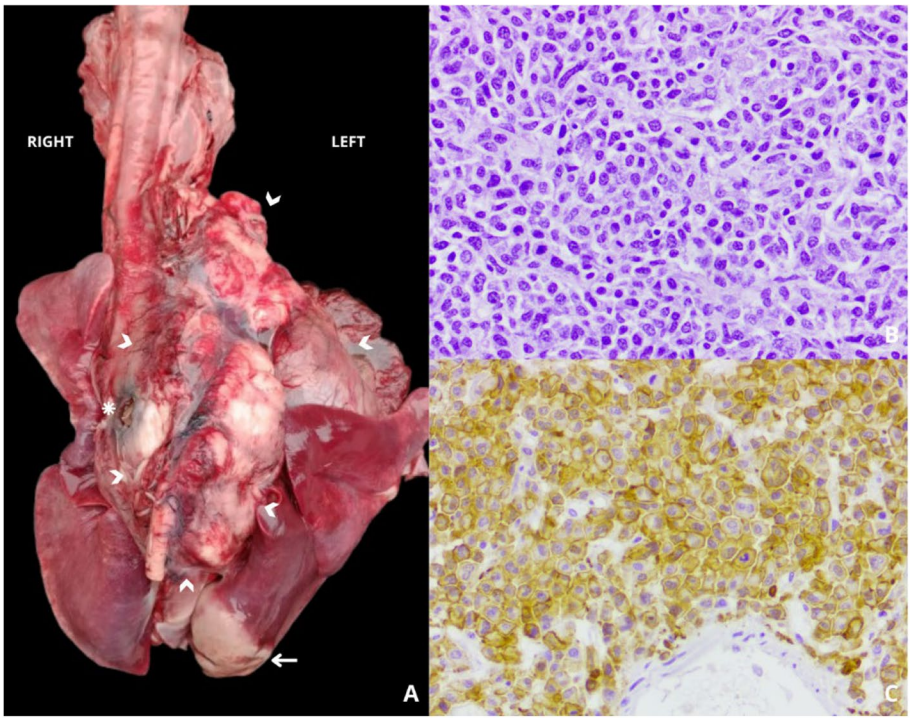

Fig. 3 Pathological evaluation of a histiocytic sarcoma in a dog. **A** Large tumor mass in the mediastinum, contiguous with the esophageal region and adhered to the adjacent lung lobes (arrowhead). In the distal esophagus, a perforation site with a hard, mineralized material inside is observed (asterisk). Additionally, a nodular area similar to the mediastinal mass is present in the left caudal lung lobe (arrow). **B** Histopathological examination showing a neoplastic proliferation of round to spindle-shaped cells, non-delimited and non-encapsulated, filling the alveolar spaces. The nuclei vary in shape from round to oval and reniform, with finely granular chromatin and single nucleoli (40× increase). **C** Immunohistochemical examination demonstrating diffuse and intracytoplasmic expression of Iba-1 (a histiocytic marker) (40× increase)

whitish area resembling the mediastinal mass was noted. Additionally, a focal perforation of the mucosa was observed within the caudal thoracic esophagus, contiguous with the aforementioned tumor mass, containing a hard, mineral-like material inside. No macroscopic alterations were observed in other organs, either within the thoracic or abdominal cavities. Table 1 presents a comparison between measurements and additional findings of mediastinal and pulmonary lesions assessed by imaging and necropsy:

During necropsy, fragments of multiple organs were collected, fixed in 10% neutral buffered formalin, and routinely processed for histopathological analysis, being stained with hematoxylin and eosin (HE).

Microscopically, a neoplastic proliferation of round-to-spindle-shaped cells was observed, non-delimited and non-encapsulated, filling the alveolar spaces. The cells were arranged in sheets and exhibited moderate, eosinophilic cytoplasm, with nuclei varying in shape from round to oval and reniform, finely granular chromatin, and single, prominent nucleoli. Additionally, severe anisocytosis and anisokaryosis, binucleation, and 32 mitotic figures per ten high-power fields (40×), frequently atypical, were noted, along with numerous cells displaying bizarre nuclei (Fig. 3B).

The same cellular pattern was observed in the esophagus, extending transmurally from the serosa, and in the cranial mediastinal lymph nodes, which were partially replaced by neoplastic proliferation. These findings were consistent with the diagnosis of a malignant round cell neoplasm, specifically pulmonary histiocytic sarcoma (HS) with esophageal and nodal metastasis being the primary differential. Tumor origin was confirmed through immunohistochemical analysis, which demonstrated strong, diffuse, and intracytoplasmic expression of ionized calcium-blinding adaptor molecule 1 (Iba-1) (a histiocytic marker) and negativity for cluster of differentiation 3 (CD3), cluster of differentiation 79 (CD79a VET), and melanoma antigen recognized by T cells 1 (Melan A/MART 1) antibodies (Fig. 3C). Considering the lesion's spread beyond the primary site and its draining lymphocenter, this case was classified as disseminated HS.

Discussion and conclusions

This report presents the occurrence of esophageal and nodal metastasis in a case of primary pulmonary histiocytic sarcoma (HS) in a dog. HS is locally invasive and frequently metastasizes to the respective draining lymph nodes [9]. Secondary implantation of primary pulmonary HS in dogs has been reported in the lung and

Table 1 Comparison measurements and additional findings of mediastinal and pulmonary lesions assessed by imaging and necropsy

Exam	Lesion location	Length (cm)	Height (cm)	Width (cm)	Additional findings
Radiography (Fig. 1)	Cranial mediastinal	16.9 cm	8.15 cm	8.8 cm	Displacement of adjacent structures; Estimation of pleural effusion volume
Ultrasonography (Fig. 2)	Cranial mediastinal	10 cm	5.7 cm	-	Quantification and characterization of pleural effusion; Identification of pulmonary lobe atelectasis; Delineation of mass margins and internal echotexture; Differentiation between mass and surrounding effusion/atelectasis
Necropsy (Fig. 3)	Cranial mediastinal/ Esophageal	14 cm	6 cm	8.5 cm	Evidence of cranial mediastinal lymph nodes and esophageal involvement; Detection of esophageal perforation and intraluminal mineralized material; Identification of additional pulmonary mass not detected on pre-mortem imaging
	Left caudal pulmonary lobe	4 cm	2.5 cm	6.2 cm	

Lesion measurements (length, height, and width) and notable findings observed on radiography, ultrasonography, and necropsy. Measurements correspond to the largest dimensions identified for each lesion in the specified anatomical location. Additional findigns summarize relevant diagnostic or pathological features noted for each modality

intrathoracic lymph nodes, as well as in distant metastatic sites, including abdominal organs [9]. Additionally, a case involving the nervous system, with metastasis to the spinous processes and spinal cord, has been documented [10]. Primary esophageal HS has been described in a dog [11], however, the occurrence of esophageal metastases, as in this case, has not been previously reported in the literature.

Esophageal involvement by histiocytic sarcomas is rarely reported in human medicine, with the few existing reports indicating a particular predilection of this neoplasm to primarily affect the gastrointestinal tract [12]. In all described cases, the individuals were young or middle-aged adults and did not present pulmonary or mediastinal neoplasms [12–14]. In the present report, the observed biological behavior was different: esophageal involvement was secondary, and the affected dog was very young. Moreover, to date, there are no descriptions of secondary esophageal involvement by this neoplasm in the canine species.

When located in the pulmonary parenchyma, HS frequently disseminates to thoracic lymph nodes, forming multiple tumor masses that tend to coalesce into a single homogeneous block [15]. Derived from macrophages and dendritic cells, these cells exhibit high migratory capacity and phenotypic plasticity, which favors tumors spread through lymphatic and hematogenous routes [15, 16]. The anatomical proximity, combined with intense thoracic dissemination and the particular migratory ability of the tumor cells, facilitated the invasion and propagation of the neoplasm to adjacent tissues such as the esophagus. Furthermore, the extensive areas of intratumoral necrosis observed in the histological examination hindered the characterization of the vascular or lymphatic pattern of metastasis.

Radiographic imaging assists in the initial localization of the lesion, guiding subsequent ultrasonographic analysis and allowing for a more targeted and detailed assessment. This contributes to suggesting the location and characteristics of the lesion, indicating the possibility of a neoplasm. Radiography is a low-cost and widely accessible method commonly used as a diagnostic tool in suspected pulmonary conditions [17, 18]. Similarly, ultrasonography is a valuable, rapid, and non-invasive tool that helps determine the cause of respiratory distress [19]. Although computed tomography (CT) is recognized as the most effective method for analyzing pulmonary parenchyma [1], its high cost and limited availability make its routine use impractical in many situations. In the present case, additional factors prevented its use, including the need for sedation, as the patient was not clinically stable enough to undergo an anesthetic procedure.

CT is more sensitive than radiography for detecting pulmonary nodules [20, 21]. In Armbrust et al. [20] study, only 41% of the nodules detected on CT were visible on radiographs. The minimum detectable size was 3 mm for radiographs and 2 mm for CT. Although these thresholds are closer than previously reported, they still demonstrate the superior sensitivity of CT, which helps explain discrepancies in nodule detection rates. Nemanic et al. [21] also note that radiographs typically detect nodules between 7 and 9 mm, generally larger than those reported in other studies [20]. In the present case, the presence of pleural effusion impaired thoracic evaluation, especially of the lung lobes, as it often causes lung collapse and complicates radiographic analysis of the pulmonary parenchyma. This limitation may explain the failure to detect the pulmonary nodule radiographically, reinforcing CT as a more sensitive diagnostic tool in such situations.

The radiographic features of primary pulmonary HS typically include a predominantly peripheral location or involvement of the entire right middle or left cranial

lung lobe, often accompanied by air bronchograms and lymphadenopathy [7]. The right middle lung lobe has been suggested as a site of predilection for primary pulmonary HS in dogs [22]; however, primary pulmonary tumors in general are more commonly reported in the peripheral regions of the caudal lung lobes [23]. In the present case, the lesion was located in the left caudal lobe, differing from the distribution pattern described by Tsai et al. [22] but aligning with the findings reported by Marolf et al. [23].

Mediastinal masses cause displacement of adjacent structures, a feature that can be identified on radiographic examination and helps differentiate pulmonary neoplasms [24]. This finding corroborates the radiographic observations (Fig. 1), given the significant involvement of the mediastinum by the neoplasm. Thus, radiographic examination indicated the possibility of a cranial mediastinal mass.

Considering the ultrasonographic characteristics observed in this case, the mediastinal mass could be differentiated from other conditions such as pneumonia-induced lung consolidations, lung lobe torsion, or abscesses [25]. Unlike radiography, the presence of pleural effusion provides a valuable acoustic window for intrathoracic ultrasonographic evaluation, facilitating the identification of changes in the thoracic wall, lungs, and mediastinum [25]. Nodular or mass-like lesions with a heterogeneous nature and well-defined margins are frequently associated with pulmonary and/or mediastinal neoplasms [26, 27].

HS lesions, which predominantly originate from interstitial dendritic cells, typically present as destructive masses with a uniform and smooth cut surface, varying in color from white/cream to tan [28]. These characteristics are similar to those observed in this case. Histologically, these lesions consist of sheets of large, pleomorphic, mononuclear, and multinucleated giant cells, with marked atypical mitoses and bizarre mitotic figures [28], findings that are consistent with the histological observations in this report.

Although these macro- and microscopic features are highly suggestive of an HS diagnosis, differentiation from other neoplasms, such as T-lymphocytes (T-cell) and B-lymphocytes (B-cell) lymphoma, requires immunohistochemical analysis. Thus, the diagnosis is supported by integrin beta chain-2 (CD18) expression and the absence of CD3 and CD79, along with Iba-1 expression, which is specific for histiocytic disorders and excludes other probable differential diagnoses [29, 30]. The expression of Iba-1 combined with the absence of CD3, CD79a VET, and Melan A antibody labeling were critical findings for confirming the diagnosis of HS in this case.

The treatment of HS is based on a combination of surgical tumor resection, when possible, along with chemotherapy and radiotherapy [1, 3]. However, the prognosis remains poor in most cases due to the high metastatic potential of the disease, with reported median survival times ranging from approximately 39 to 406 days [3]. In this case, disease progression was already underway, contributing to its deleterious course and ultimately leading to the animal's death. The severity of the condition was initially suggested by the association between clinical examination and imaging findings and was confirmed at necropsy, which revealed involvement of multiple organs, including the lung, esophagus, and lymph nodes.

The aggressive nature of the disease and its high metastatic potential led to an extensive mediastinal lesion originating from the primary site in the lungs, with involvement of the cranial mediastinal and tracheobronchial lymph nodes. However, the occurrence of esophageal metastases is considered rare, highlighting the uniqueness of this case and supporting the potential for its occurrence. Given the spread of the lesion beyond the primary site and the drainage lymphocenter, this case was classified as disseminated HS.

As limitations, given that this is a single-case study, the findings observed may not be extrapolated to the broader canine population. Furthermore, a pre-mortem biopsy was not performed due to the patient's clinical instability, and for the same reason, CT was not undertaken. This examination could have allowed a comprehensive assessment of the lesion and a more precise characterization of the structures and organs affected by the neoplasm. These constraints limited diagnostic confirmation prior to necropsy. Finally, it is worth considering, albeit briefly, whether an earlier diagnosis might have influenced the clinical course or the outcome of the case, underscoring the importance of timely investigation.

This manuscript presents a compelling case of primary pulmonary HS with unusual esophageal metastasis. The multimodal diagnostic approach and the emphasis on the limitations of imaging in emergency settings are strengths, making this a valuable contribution to the veterinary oncology literature. Thoracic radiography and ultrasonography, as accessible and rapidly applicable diagnostic tools, played an essential role in raising the initial suspicion of neoplasia, enabling lesion characterization and assisting in clinical prognosis determination, thereby highlighting their importance in early diagnostic approaches. When used together, these techniques complement each other and enhance diagnostic accuracy. The significance of histopathological and immunohistochemical evaluation in confirming the neoplasm is also emphasized.

Abbreviations

%	Percentage
°C	Degrees Celsius

B-cell	B lymphocyte
CD18	Integrin beta chain-2
CD79	Cluster of differentiation 79
Cm	Centimeter
CT	Computed tomography
DV	Dorsoventral
GE	General Electric
HE	Hematoxylin and eosin
HS	Histiocytic sarcoma
Iba-1	Ionized calcium-binding adaptor molecule 1
Kg	Kilogram
kV	Kilovolt
mAs	Milliampere-seconds
Melan A/MART-1	Melanoma antigen recognized by T cells 1
mL	Milliliter
mm^3	Cubic millimeter
MHz	Megahertz
T-cell	T lymphocyte

Acknowledgements
Not applicable.

Authors' contributions
AVH conceptualized the report and manuscript. FABS was the clinical lead of the case and described part of the report. AVH and RB acquired the radiographic and ultrasonographic images and provided their descriptions in the text. FABS and CKNC were responsible for the necropsy examination and the interpretation of the histological images. LSS conceptualized the manuscript draft. LSS, CB, FSF, IKCS, and RP reviewed the manuscript.

Funding
There was no funding.

Data availability
Not applicable.

Declarations

Ethics approval and consent to participate
The data used in the present case report were obtained with the approval and authorization from the responsible parties.

Consent for publication
The authorization from the responsible parties was obtained for publication.

Competing interests
The authors declare no competing interests.

Author details
[1]Postgraduate Program in Veterinary Medicine, Universidade Federal de Santa Maria (UFSM), Hospital Veterinário Universitário (HVU), Av. Roraima, 1000, Prédio 97, Santa Maria, Rio Grande Do Sul 97105-900, Brazil
[2]Postgraduate Program in Veterinary Sciences, Universidade Estadual Paulista, Rua Prof. Paulo Donato Castellane, S/N - Vila Industrial, Jaboticabal, São Paulo 14884-900, Brazil
[3]Residency Program in Health Professional Area – Veterinary Medicine, UFSM, Av. Roraima, 1000, Prédio 97, HVU, Santa Maria, Rio Grande Do Sul 97105-900, Brazil
[4]Department of Imaging Diagnostic, UFSM. Av. Roraima, HVU, Prédio 97, Santa Maria, Rio Grande Do Sul 100097105-900, Brazil
[5]Department of Large Animals Clinic, UFSM. Av. Roraima, HVU, Prédio 97, Santa Maria, Rio Grande Do Sul 100097105-900, Brazil

Received: 26 March 2025 / Accepted: 10 September 2025
Published online: 25 November 2025

References

1. McPhetridge JB, Scharf VF, Regier PJ, Toth D, Lorange M, Tremolada G, et al. Distribution of histopathologic types of primary pulmonary neoplasia in dogs and outcome of affected dogs: 340 cases (2010–2019). JAVMA. 2021;260(2):234–43.
2. Affolter VK, Moore PF. Localized and disseminated histiocytic sarcoma of dendritic cell origin in dogs. Vet Pathol. 2002;39(1):74–83.
3. Dervisis NG, Kiupel M, Qin Q, Cesario L. Clinical prognostic factors in canine histiocytic sarcoma. Vet Comp Oncol. 2017;15(4):1171–80.
4. Erich SA, Dobson JM, Teske E. Comparison of the clinical characteristics of histiocytic sarcoma in Bernese Mountain Dogs and Flat-Coated Retrievers. Vet Sci. 2022;9(9):498.
5. Lenz JA, Furrow E, Craig LE, Cannon CM. Histiocytic sarcoma in 14 miniature schnauzers - a new breed predisposition? J Small Anim Pract. 2017;58(8):461–7.
6. Latifi M. Clinical outcomes in dogs with localized splenic histiocytic sarcoma treated with splenectomy with or without adjuvant chemotherapy. J Vet Intern Med. 2020;34(6):2645–50.
7. Barrett LE, Pollard RE, Zwingenberger A, Zierenberg-Ripoll A, Skorupski KA. Radiographic characterization of primary lung tumors in 74 dogs. Vet Radiol Ultrasound. 2014;55(5):480–7.
8. Lobaczewski A, Czopowicz M, Moroz A, Mickiewicz M, Sapierzynski R, Tarka S, et al. Integrated basic heart and lung ultrasound examination for the differentiation between bacterial pneumonia and lung neoplasm in dogs - a new diagnostic algorithm. Animals (Basel). 2022; 12(9):1154.
9. Marlowe KW, Robat CS, Clarke DM, Taylor A, Touret M, Husbands BD, et al. Primary pulmonary histiocytic sarcoma in dogs: a retrospective analysis of 37 cases (2000–2015). Vet Comp Oncol. 2018;16(4):658–63.
10. Nemoto Y, Nakaichi M, Sakurai M, Itamoto K, Morimoto M, Horikirizono H, et al. Histiocytic sarcoma with spinal necrosis in a dog with progressing non-ambulatory tetraparesis. Open Vet J. 2023;13(3):394–9.
11. Trindade-Gerardi AB, Silveira CA, Duz J, Silva ITCP, Guim TN, Pavarini SP, et al. First description of a primary esophageal histiocytic sarcoma in a dog. Top Companion Anim Med. 2024;59:100856.
12. Philip DSJ, Sherief A, Narayanan G, Nair SG, Av J. Histiocytic sarcoma: Clinical features and outcomes of patients treated at a tertiary cancer care center. Cureus. 2022;14(6):e25814.
13. Comesaña Castellar C, Payeras Capo MA, Fernández García J, Calvo Martínez C, Ramis Estelrich MD, Díaz Molina RJ, et al. Histiocytic sarcoma of the esophagus. Rev Esp Enferm Dig. 2023;115(10):583–4.
14. Pakravan A, Bhatia R, Oshima K, Chen G, Fesler M, Prather C, et al. Histiocytic sarcoma: the first reported case of primary esophageal involvement. Am J Gastroenterol. 2014;109(2):291–2.
15. Caswell JL, Williams KJ. Respiratory system. In: Maxie MG, editor. Jubb, Kennedy & Palmer's Pathology of Domestic Animals, vol. 2. 6th ed. Elsevier; 2015. p. 495–502.
16. Fulmer AK, Mauldin GE. Canine histiocytic neoplasia: an overview. Can Vet J. 2007; 48(10):1041–1043, 1046–1050.
17. Gefter WB, Post BA, Hatabu H. Commonly missed findings on chest radiographs: causes and consequences. Chest. 2023;163(3):650–61.
18. Masseau I. Canine and Feline Lung. In: Seiler GS, Thrall DE, editors. Thrall's Textbook of Veterinary Diagnostic Radiology. 8th ed. St. Louis, Missouri: Elsevier; 2025. Ch. 36, p.3056–3199.
19. Oricco S, Medico D, Tommasi I, Bini RM, Rabozzi R. Lung ultrasound score in dogs and cats: a reliability study. J Vet Intern Med. 2024;38(1):336–45.
20. Armbrust LJ, Biller DS, Boudrieau RJ, et al. Comparison of three-view thoracic radiography and computed tomography for detection of pulmonary nodules in dogs with confirmed neoplasia. J Am Vet Med Assoc. 2012;240(9):1088–94.
21. Nemanic S, London CA, Wisner ER. Comparison of thoracic radiographs and single breath-hold helical CT for detection of pulmonary nodules in dogs with metastatic neoplasia. J Vet Intern Med. 2006;20(3):508–15.
22. Tsai S, Sutherland-Smith J, Burgess K, Ruthazer R, Sato A. Imaging characteristics of intrathoracic histiocytic sarcoma in dogs. Vet Radiol Ultrasound. 2012;53(1):21–7.
23. Marolf AJ, Gibbons DS, Podell BK, Park RD. Computed tomographic appearance of primary lung tumors in dogs. Vet Radiol Ultrasound. 2011;52(2):168–72.
24. Ruby J, Secrest S, Sharma A. Radiographic differentiation of mediastinal versus pulmonary masses in dogs and cats can be challenging. Vet Radiol Ultrasound. 2020;61(4):385–93.
25. Larson MM. Ultrasound of the thorax (noncardiac). Vet Clin North Am Small Anim Pract. 2009;39(4):733–45.
26. Lin CH, Lo PY, Lam MC, Wu HD. Usefulness of Chest Ultrasonography in Predicting Diagnosis in Non-emergency Small Animal Patients With Lung Parenchymal and Pleural Disease. Front Vet Sci. 2020;7:616882.

27. Patterson MM, Marolf AJ. Sonographic characteristics of thymoma compared with mediastinal lymphoma. J Am Anim Hosp Assoc. 2014;50(6):409–13.
28. Moore PF. A review of histiocytic diseases of dogs and cats. Vet Pathol. 2014;51(1):167–84.
29. Flecher MC, Nascimento NT, Reys MP, Gorza LL, Souza MCC, Horta RS. Periarticular histiocytic sarcoma in a French bulldog. Braz J Vet Pathol. 2024;17(1):39–20.
30. Ramos-Vara JA, Borst LB. Immunohistochemistry: Fundamentals and Applications in Oncology. In: Meuten DJ, editor. Tumors in Domestic Animals. 5th ed. Ames, Iowa: John Wiley & Sons Inc; 2016. Ch. 3, p. 44–87.

Publisher's Note